Precision Agriculture Using Hyperspectral Remote Sensing and GIS

Haluk Cetin[1], John T. Pafford[2] and Tom G. Mueller[3]
[1]The Mid-America Remote Sensing Center, Haluk.Cetin@MurrayState.edu
Murray State University, Murray, KY 42071 USA
[2]The Department of Geosciences, jpaffrd2@hotmail.com
Murray State University, Murray, KY 42071 USA
[3]The Department of Plant and Soil Sciences, mueller@uky.edu
University of Kentucky, Lexington, KY 40546-0091 USA

Abstract-**The objectives of this study were to utilize hyperspectral Real-time Data Acquisition Camera System (RDACS-3; 120 bands and 2x2m pixel resolution) imagery to examine spectrally sensitive regions for the detection of Nitrogen (N) deficiency in corn and to determine whether hyperspectral and/or multispectral remote sensing, and Geographic Information Systems (GIS) could be used to improve N management through early detection of vegetation stress. Several N studies with varying rates of N fertilizer were conducted in Calloway County, Kentucky, USA to examine the relationships between crop biophysical variables and crop stress. Multi-temporal Hyperspectral RDACS data were collected for the study area. Logistic Regression and Multiple Linear Regression techniques identified spectrally sensitive regions in blue, red and near-Infrared wavelength regions of the Electromagnetic spectrum. These regions were modeled and compared with traditional hyperspectral and multispectral techniques. The results of these comparisons revealed the greater effectiveness of hyperspectral imagery feature selection in the shorter red region over the typical Normalized Difference Vegetation Index approach. Hyperspectral imagery with high spectral and spatial resolutions offers distinct advantages over multispectral data for early detection of stress in vegetation. The application of high resolution remote sensing in agriculture should improve fertilizer N use efficiency and reduce N losses to the environment.**

I. INTRODUCTION

In the incident solar spectrum, the spectral characteristics of a living green leaf depend primarily on pigmentation, leaf structure, and water content. Chlorophyll exhibits a predominant influence on leaf spectral responses to plant stress in the visible and far-red spectra. The chlorophyll in a healthy plant will strongly absorb blue and red light while reflecting relatively high proportions of green and infrared light. Often, leaf chlorophyll content decreases when plants are affected by some environmental stressor. As a result, absorption of visible light decreases, reflectance is increased, and chlorosis, or a general yellowing of leaves, may be observed. Remote sensing systems can often provide earlier and more comprehensive detection of such stress symptoms than visual observation in the field. In the past, studies concerning plant stress detection have utilized vegetation indices such as the Normalized Difference Vegetation Index (NDVI) obtained from multispectral data. However, hyperspectral imagery with high spectral and spatial resolutions offers distinct advantages over multispectral imagery for early detection of stress in vegetation. Statistical evaluative procedures and feature extraction techniques utilizing extraction of useful spectral regions for stress detection offer effective methods of depicting stressed regions. Also, the relationships between crop biophysical variables and discrete spectral regions should indicate wavelengths particularly sensitive to vegetative stress.

The large division of channels allows for selection of bands that provide the greatest contribution of data to a particular task. Eliminating spectral regions that do not contribute to the model's overall effectiveness allows for greater accuracy of results. The increased spectral resolution of hyperspectral imagery creates a challenge in identification of useful spectral regions for a given application. Researchers have identified these areas of interest through numerous quantitative methods of linear regression [1, 2], derivative based analysis [3, 4], Discriminant Function Analysis [2] and spectral mixture analysis [5,6,7]. Also assessment of vegetation stress [8, 9, 10], soil conditions [11] and nitrogen/other organic matter deficiencies [12] have been important. Ultimately, the challenge stems from the need to reduce the dimensionality of the large number of band on band combinations and permutations available from hyperspectral data and create a less cumbersome dataset.

The NDVI, a most commonly used vegetation index for identifying healthy vegetation in multispectral applications, has been applied in hyperspectral investigations but has not been accepted as the most effective method for identifying stress in crops. More frequently, research methodology in hyperspectral cases has relied on quantitative comparisons of numerous indices such as the Transformed Soil Adjusted Vegetation Index (TSAVI), the Derivative-based Green Vegetation Index (DGVI) and the Photosynthetic Reflectance

0-7803-8977-8/05/$20.00 ©2005 IEEE.

index (PRI), to identify the best method in a given application [2, 3, 13, 14].

The objectives of this study were to utilize hyperspectral Real-time Data Acquisition Camera System (RDACS-3) imagery with 120 bands and 2x2m pixel resolution to examine spectrally sensitive regions for the detection of Nitrogen (N) deficiency in corn and to determine whether hyperspectral and/or multispectral remote sensing, and Geographic Information Systems (GIS) could be used to improve N management through early detection of vegetation stress. Several N studies with varying rates of N fertilizer were conducted in Calloway County, Kentucky, USA to examine the relationships between crop biophysical variables and crop stress.

II. Study Area

As part of several hyperspectral remote sensing studies including a National Aeronautics and Space Administration (NASA)/Kentucky EPSCoR project and a Cooperative State Research, Education, and Extension Service (CSREES) program of the United States Department of Agriculture/University of Kentucky project, our study focused on establishing a method for early detection of N deficiency in agricultural crops using hyperspectral and multispectral remote sensing. Ponderosa Farms are located approximately 18 kilometers southwest of Murray in Calloway County, Kentucky, USA (Fig. 1). The land cover types and climate at Ponderosa Farms are ideally suited to experimental studies with a temperate climate, fertile soils, gentle rolling terrain and even distribution of precipitation throughout the year. Crop types grown in numerous fields at Ponderosa Farms include corn, soybeans and winter wheat, primarily. This particular study focused on an area of the Farms known as Suggs field, which contained a corn crop in development. Suggs field had been administered differing treatments of N, ranging from 0 to 55 kg/ha.

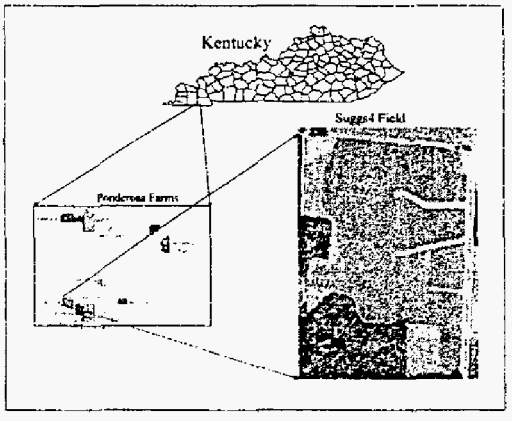

Figure 1. Location map of the study area, Ponderosa Farms, Kentucky, USA

III. Methodology

Imagery utilized in this project included both hyperspectral and multispectral scenes of the area encompassing Suggs field (Fig. 2). RDACS-3 hyperspectral imagery acquired on June 19 and August 14, 2001 was analyzed, as well as a multispectral IKONOS image acquired on August 17, 2001. The RDACS-3 imagery yielded a total of 120 spectral bands with 2 x 2 meter resolution, while the IKONOS scene contained 4 bands. Also, a high resolution 0.5 x 0.5 meter multispectral image acquired on August 14, 2001 with 4 bands was available for analysis. The dates of acquisition for this imagery depicted a corn crop in both relatively early and late stages of development. Geographic Information Systems (GIS) data used included planned N application zones, field elevation data, crop yields and as-applied N treatment rates (Fig. 3). Previously gathered field spectra of various surfaces (Fig. 4) were utilized to compute radiance-to-reflectance conversion for the hyperspectral images in the area (Fig. 5).

A variable rate N-rate experiment was conducted in Ponderosa Farms including the Suggs field. The soils in the experimental area were generally developed in loess parent material and had restrictive layers (fragipans), which varied in depth. Approximately 40 kg/ha N fertilizer was applied prior to planting. The corn was side dressed with varying rates of N (0, 30, 40, 50, and 55 kg N ha^{-1}) at the V5 growth stage corn stage using ammonium nitrate (34-0-0). RDACS data were collected in May, June and August of 2001. IKONOS data were available only for August 2001. Thus, only August data were used herein for IKONOS versus RDACS comparisons.

A. Preprocessing

In order to prepare the hyperspectral imagery for data reduction, it was necessary to complete several stages of preprocessing including rectification, creation of a subset image of the study area, and examination for noise removal. The raw data scenes acquired by RDACS-3 on June 19 and August 14, 2001 were rectified to Universal Transverse Mercator (UTM), North American Datum (NAD) 1927 for further processing. After both images had been accurately rectified, they were subset to the desired study area.

Since sensor noise can be a problem in scanning systems, the dark current images from the two scenes were examined. The dark current image displays noise attributable to overheating of the sensor chip when hot pixels become visible on a test scan made with the sensor optics obscured. In this application, examination of the dark current images revealed little if any bad pixels in the imagery. Therefore, it was not deemed necessary to subtract the dark current images from the two scenes.

Methods for removal of atmospheric and solar effects from hyperspectral imagery are varied. However, use of a particular method relies upon whether the researcher has previously measured field spectra available and/or a priori knowledge of a given area. Calibration methods such as Atmospheric Removal Program (ATREM) rely on the use of particular narrow spectral regions that correlate to atmospheric vapor [16]. Other procedures such as the Flat Field technique utilize a spectrally flat region's signature to subtract from the image on a pixel by pixel basis. However, when field measured spectra are available the Empirical

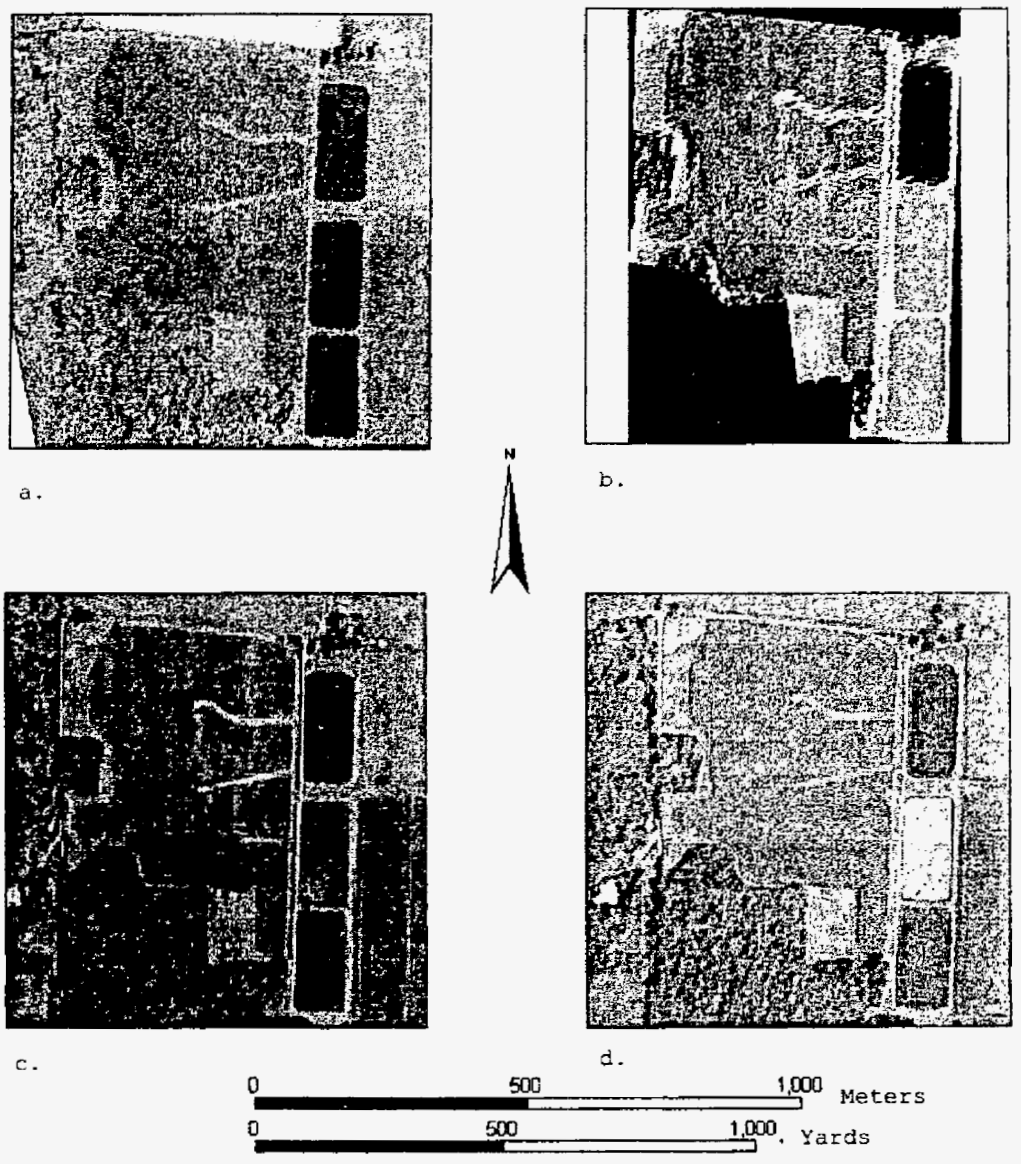

Figure 2. False color composites of Suggs field, Ponderosa Farms, Kentucky:
a.) RDACS-3 June 19, 2001 (Red=828 nm; Green=708 nm; Blue=558 nm)
b.) RDACS-3 August 14, 2001 (Red=828 nm; Green=708 nm; Blue=558 nm)
c.) IKONOS August 17, 2001 (Red=805 nm; Green=665 nm; Blue=551 nm), (Copyright: Space Imaging)
d.) Multispectral August 14, 2001 (Red=830 nm; Green=660 nm; Blue=560 nm)

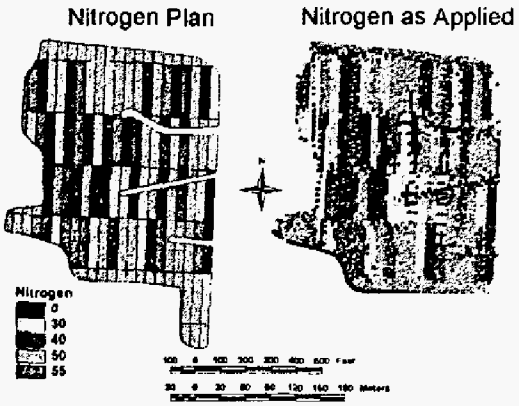

Figure 3. Planned nitrogen application zones and as-applied nitrogen treatment rates

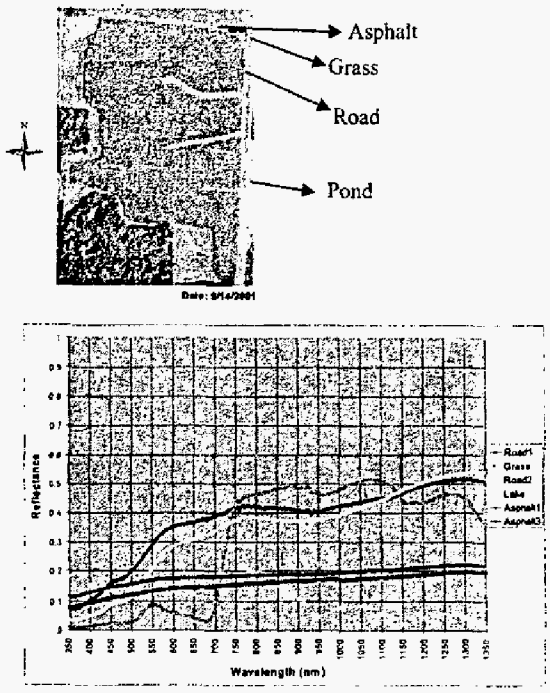

Figure 4. Ground spectral data collection locations and spectra of the various surfaces used in the radiance-to-reflectance conversions

Figure 5. August 14, 2005 field pictures

Line Calibration (ELC) method can be used to derive apparent reflectance. The ELC method is a regression technique that forces spectral data in a scene to match field measured spectra.

The linear regression model is used for each band to produce digital number reflectance. The equation (1) illustrates how the empirical line values are calculated [17].

$$\textit{Reflectance (Field Spectrum)} = \textit{gain} \times \textit{radiance (input data)} + \textit{offset} \quad (1)$$

The ELC method was utilized for the two RDACS-3 images by pairing spectra from imagery targets such as asphalt roads (dark target), gravel roads (light target), corn, water or grass with previously measured spectroradiometer data from the study area. The endmembers or spectral signatures of these materials derived from the imagery were then output to an ASCII (American Standard Code for Information Interchange) file, paired with the field spectra in Excel and input into ENVI's ELC program.

B. Data Reduction

After preprocessing of the hyperspectral imagery was completed, the task then turned to reduction of the overwhelmingly large spectral component of the data. Since hyperspectral imagery provided high spectral resolution, it was necessary for the researcher to use some type of methodology to discriminate useful spectral regions or "features". The method chosen for this application was a random point sampling approach. Although more direct approaches to spectral data such as Principal Components Analysis have been utilized in the past, it was deemed counterproductive for identification of specific narrow stress sensitive spectral regions. Therefore, in order to investigate these regions, pixel values from random samples for treatment zones (0, 30, 40, 50 and 55 kg/ha N) were extracted and used in statistical analysis. The random point procedures involved conversion of the vector N treatment plan to a thematic raster layer where 20 random points were generated per treatment level. These 20 points were further reduced to

10 by eliminating points that exhibited either overlap or location on or near the edges between treatment zones. As a result, a total of 50 sample points, 10 per treatment from the five application rates, were chosen for analysis. Groups of pixels surrounding these random points were then subset to incorporate greater variability for each treatment level. These sample pixels from the imagery were then converted to ASCII values for further processing.

C. Statistical Analysis

One of the primary goals of this research was to identify specific stress sensitive spectral wavelengths from the 120 different channels. In order to accomplish this, a quantitative approach was taken to eliminate non relevant data. The methods employed in this analysis included two-way Analysis of Variance (ANOVA), Logistic regression (LR), and Multiple Linear regression (MLR).

As an initial step, treatments and wavelength were paired in a two-way ANOVA model that examined the variances of reflectance at each level in the model and tested for significant interaction between N treatment and wavelength. After interaction was tested, the main effect of N treatment was examined for significant differences.

To further identify significant stress sensitive regions, LR was employed. LR assumes the fact that the dependent variable is dichotomous, in that a model is created where 0 represents failure, a non-event, and 1 represents a success, or an event. The overall model seeks to predict the probability of an event through use of the values of a set of independent predictor variables using a Logistic function [18]. The Logistic function in regression is shown in (2).

$$E(Y) = \frac{1}{1 + \exp\left[-\left(\beta_0 + \sum_{j=1}^{k} \beta_j X_j\right)\right]} \quad (2)$$

Where: E(Y) is the probability that Y=1

Therefore, four models were produced, 0 vs. 30 kg/ha, 0 vs. 40 kg/ha, 0 vs. 50 kg/ha and 0 vs. 55 kg/ha, including all 120 channels in the model as independent predictor variables. The 0 kg/ha treatment was viewed as control or non-event pixels and compared with treated pixels at 30, 40, 50 or 55 kg/ha. Computational restraints on the size of the data required that the total number of bands in each model be limited to 60. Stepwise variable selection was used to identify the most significant bands from the two models and create a final model for analysis.

Following stepwise model creation, physical variables including elevation and soil type were added to the model to test for significance. The results derived from analysis of the four models were then tested for classification accuracy using an independent set of observations.

The relationships between biophysical variables including effective Leaf Area Index (eLAI), estimated chlorophyll content and crop yield and reflectance at each treatment level were investigated through the use of multiple linear regression procedures. This was accomplished by modeling the biophysical variables as dependent, while the spectral wavelengths and their associated reflectance values at a given treatment were modeled as predictor variables.

D. Stress Sensitivity Index Modeling

Features identified from regression techniques as significant in stress detection were evaluated and utilized to create several stress sensitivity index models. These models were fashioned after the traditional NDVI methodology, where the contrast between red and NIR depicts healthy vegetation. However, the models created for this application were not limited to use of features from the red and NIR. Also, SAVI style stress images were created.

In order to compare the results of the aforementioned models with that of traditional NDVI and SAVI indices, NDVI and SAVI images were created for 1.) RDACS-3 scenes, utilizing spectral channels deemed applicable by [13], 2.) IKONOS and 3.) multispectral camera images. Difference images were generated for each dataset to highlight improvements of the stress sensitivity indices over that of traditional NDVI and SAVI results.

IV. Results and Discussion

Initially, a two-way ANOVA was performed to attempt to identify particular spectral wavelengths that displayed significant reflectance difference based on treatment. The ANOVA results revealed that the overall trend did not indicate significant interaction between N treatment and wavelength (p value = 0.0528); however, the apparent borderline significant p value did point to possible interaction in specific spectral regions. Therefore, Tukey pairwise comparison procedures were used to compare levels of treatment at a given wavelength. However, computational restraints did not allow this analysis to be successfully conducted and preliminary results based on a smaller model indicated that because of the large number of observations available, all comparisons were shown to be statistically significant.

As an alternative approach, Logistic Regression was used to model the control group (0 kg/ha N) against a given treatment (30, 40, 50 or 55 kg/ha N). In effect, four models were constructed, one for each level of N. Stepwise variable selection results are shown in Table I.

For the model 0 kg/ha vs. 30 kg/ha N, the spectral regions indicated with the highest significance and odds ratio estimates were at 483 nm (blue), 510 nm (green), 636 nm (red) and 696 (red/NIR edge). Interestingly, at 483 nm the odds for a pixel belonging to the treatment class were 4.5 times greater than non- treatment for a single unit change at 483 nm, with all other wavelengths held fixed. Also, at 510 nm and 636 nm the odds were shown to be increased by 2.5 and 2.6, respectively.

At 40 kg/ha N versus control, the most significant spectral regions indicated were at 636 nm, 639 nm, 672 nm and 735 nm. The 636 nm region was shown to be particularly

TABLE I

LOGISTIC REGRESSION MODEL RESULTS

	Model 1 *0 vs. 30 kg/ha*	Model 2 *0 vs. 40 kg/ha*	Model 3 *0 vs. 50 kg/ha*	Model 4 *0 vs. 55 kg/ha*
Significant Regions (nm)	483,510,525 567,588,636 639,696 813	522,531,636, 639,672,699, 705,711,720, 723,735,789	540,573,636 645,708,717 750,771,783	483,657,711 723,747,759 753
Somer's D	0.855	0.983	0.94	0.989
Odds Ratio Estimates (nm)	483 = 4.575 510 = 2.503 525 = 1.569 567 = 0.658 588 = 0.651 636 = 2.619 639 = 0.661 696 = 0.638 813 = 0.925	522 = 0.20 531 = 0.12 636 = 40.48 639 = 3.45 672 = 6.95 699 = 0.14 705 = 0.13 711 = 0.29 720 = 0.43 723 = 2.09 735 = 1.82	540 = 0.514 573 = 0.393 636 = 2.944 645 = 1.957 708 = 0.670 717 = 0.790 750 = 1.134 771 = 0.916 783 = 1.083	483 = 6.156 657 = 3.789 711 = 0.618 723 = 0.567 747 = 1.292 750 = 1.494 753 = 1.377

responsive to this level of treatment with an odds ratio estimate 40.5 times greater than other regions held constant. Even at 639 nm, the odds ratio was shown to be increased by 3.4 times. The high level of significance and extremely high odds ratios indicated that this region in early red was very sensitive to stress.

At 50 kg/ha versus control, spectral regions indicated with the highest significance were 540 nm, 573 nm, 636 nm, 645 nm and 708 nm. Odds for differentiating treatment at 50 kg/ha from control with other regions held constant were greater at 636 nm (2.9) and 645 nm (1.9) in the red region, than in the IR region. Also, at 55 kg/ha versus control the region with the highest odds ratios was blue (483 nm), and red (657 nm), while the model utilized the majority of predictor variables from the IR region.

Overall, the results of Logistic regression modeling indicated that the red region, especially at or near 636 to 639 nm, was a consistently significant spectral region with higher odds for differentiating treatment from control pixels with other spectral regions held constant. It was also apparent that regions in blue (471 nm, 483 nm, 486 nm and 492 nm) also displayed significant ability to distinguish treatment levels. In particular, 483 nm was shown to be important in modeling both low and high treatment levels of N.

In order to visually discriminate stressed regions from healthy vegetation, it was necessary to not only indicate which spectral regions were particularly sensitive, but also create a method for displaying these differences. Therefore, crop biophysical variable correlations with wavelength were compared on a treatment by treatment basis. The reason for this methodology stemmed from the desire to include spectral regions in the model which displayed high correlations at a given treatment for all crop biophysical variables.

Creation of stress sensitive models dictated the inclusion of spectral regions highly correlated with crop biophysical variables and those shown to be significant in differentiating treatment from control (0 kg/ha N) in Logistic procedures. Both 483 nm and 636 nm were indicated as significant in Logistic regressions, while 639 nm and 750 nm were indicated through correlations with crop biophysical variables. As a result, 483 nm (blue), 636 nm (red) and 639 nm (red) were each used to ratio separately with 750 nm (Fig. 6) (Table 2). The images resulting from the three proposed models were then compared with an NDVI image created from the model proposed by [13] (Fig. 7). When the

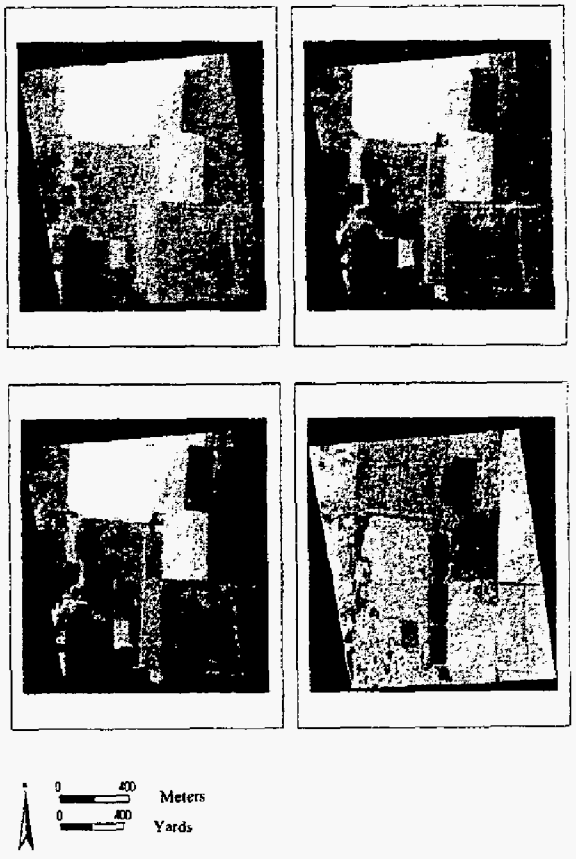

Figure 6. Suggs field panchromatic images of spectral regions identified as stress sensitive: a.) 483 nm; b.) 636 nm; c.) 639 nm; d.) 750 nm

TABLE II
MODELS FOR STRESS SENSITIVE INDICES

	Model 1	Model 2	Model 3	Model 4
Spectral Regions	750 nm 636 nm	750 nm 483 nm	750 nm 639 nm	777 nm 663 nm

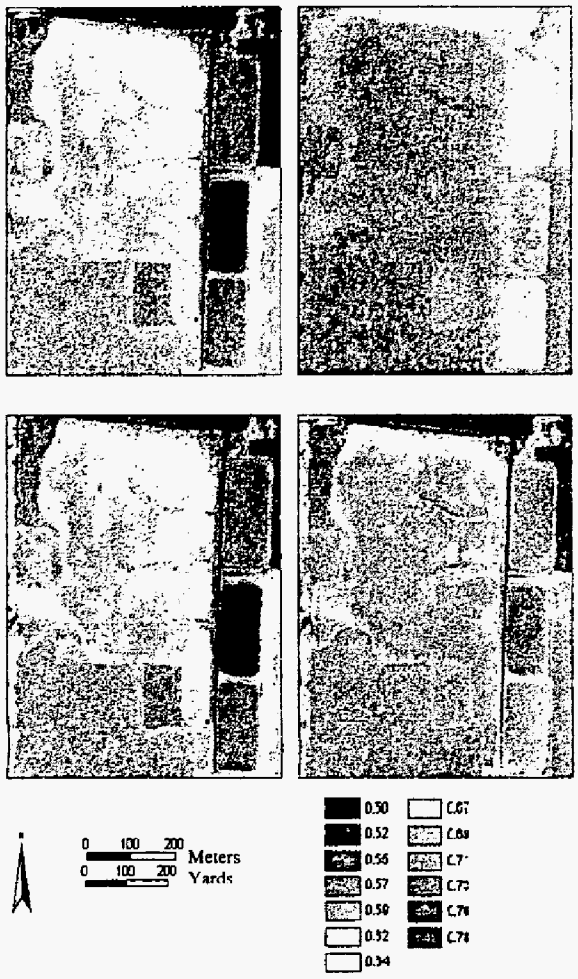

Figure 7. NDVI model images for Suggs field
a) Model 1; b.) Model 2; c) Model 3; d.) Model 4

models were compared on the basis of strongest relationship with eLAI, Model 3 demonstrated the highest overall correlation. When examining model correlations with chlorophyll, Model 2 yielded the best results. Overall, relationships between stress models and chlorophyll were strongest at either high stress (0 kg/ha N) or healthy (55 kg/ha N) regions. Model 3 was demonstrated as having the best correlation with crop yield. With the exception of crop yield, Model 4 demonstrated the lowest overall correlation.

Detection of early stress in crops is dependent upon reliance of extremely sensitive and accurate spectral data. This research has shown the advantages of hyperspectral imagery over traditional multispectral NDVI depictions of crop stress. Also, it was shown that stress induced by decreases in leaf chlorophyll is best detected with hyperspectral imagery through use of spectral regions in the shorter red wavelength region (636-639 nm) rather than the middle red region as proposed by [13]. This region was shown to exhibit consistently high correlations with crop biophysical variables across a broad spectrum. In contrast to the shorter green region, the near-infrared region displayed high correlations at 750 nm; however, the spectral range of high correlations was extremely narrow and highly sensitive to change in chlorophyll content. Also, since soil influence was a factor in early crop development, models benefited from the incorporation of a SAVI style soil adjustment factor. The most effective method of this adjustment was utilization of the eLAI image as a measure of soil influence rather than an arbitrary L factor. As a result, it was demonstrated that differing levels of crop health could be readily identified utilizing feature selection.

Examination of the relationships between crop biophysical variables and crop stress revealed several trends. As a general rule, areas displaying the highest degree of vegetative vigor at the 55 kg/ha N treatment generated the lowest correlation with eLAI, chlorophyll and yield. For both eLAI and yield, correlations with the visible spectra were almost non-existent and did not increase until near-infrared, peaking at 750 nm. eLAI was shown to display the strongest relationship with stressed regions, especially throughout early red where correlation values rose for 0 kg/ha to 40 kg/ha and thereafter rapidly fell from 50 kg/ha to 55 kg/ha N. Healthy regions represented by 50 and 55 kg/ha N for eLAI demonstrated stronger relationships with near-infrared rather than visible. This behavior demonstrated that varying conditions of plant stress, witnessed through chlorophyll depletion, are most evident in the spectral sensitive late green and early red regions. Unfortunately, correlations between estimated chlorophyll and treatment levels were weak, probably as a result of the lack of a field adjustment. However, 0 kg/ha N areas displayed the highest overall relationship with chlorophyll, especially near the red edge from 702 to 708 nm. Yield demonstrated a dramatically higher correlation with 50 kg/ha N, centering near 669 nm, than when compared with other treatments. 0 kg/ha N areas also displayed the highest correlation values with 669 nm for yield. Perhaps the higher correlation for yield with 50 kg/ha depicted an ideal level of N application for a healthy and productive corn crop. Overall, the 50 kg/ha N treatment displayed the highest correlation values for both eLAI and yield.

ACKNOWLEDGMENT

We would like to thank the Scientific Data Purchase Program, NASA Earth Science Applications Directorate for providing IKONOS data, ITD Spectral Visions for collecting and providing the RDACS data, and Ag Connections for providing some of the ground data. This study was supported by the Kentucky NASA-EPSCoR Research Grant (NCC5-571) and the CSREES program of the U.S. Department of Agriculture/University of Kentucky.

REFERENCES

[1] P.S. Thenkabail, R. B. Smith, and E. DePauw, "Hyperspectral Vegetation Indices for determining agricultural crop characteristics," Remote Sensing of Environment, vol. 71, pp. 158-182, 2000.

[2] P.S. Thenkabail, R. B. Smith, and E. DePauw, "Evaluation of Narrowband and Broadband Vegetation Indices for Determining Optimal Hyperspectral Wavebands for Agricultural Crop Characterization," AVIRIS Airborne Geoscience Workshop Proceedings, 2001 http://www.yale.edu/ceo/Projects/swap/pubs/veg_ind_text.pdf.

[3] Z. Chen, C. D. Elvidge, and D. P. Groenveld, "Discrimination of Green Vegetation Cover Using a High Spectral Resolution Vegetation Index," AVIRIS Airborne Geoscience Workshop Proceedings, 1996, ftp://popo.jpl.nasa.gov/pub/docs/workshops/96_docs/4.pdf

[4] S. D. Stearns, B. E. Wilson, and J. R. Peterson, "Optimal Band Selection for Dimensionality Reduction of Hyperspectral Imagery," AVIRIS Airborne Geoscience Workshop Proceedings, 1993, ftp://popo.jpl.nasa.gov/pub/docs/workshops/93_docs/43.pdf.

[5] C. A. Bateson, G. P. Asner, and C. Wessman, "Incorporating Endmember Variability into Spectral Mixture Analysis through Endmember Bundles," AVIRIS Airborne Geoscience Workshop Proceedings, 1998, ftp://popo.jpl.nasa.gov/pub/docs/workshops/98_docs/6.pdf.

[6] W. J. Okin, G. S. Okin, D. A. Roberts, and B. C. Murray, "Multiple Endmember Spectral Mixture Analysis: Endmember Choice in an Arid Shrubland," AVIRIS Airborne Geoscience Workshop Proceedings, 1999, ftp://popo.jpl.nasa.gov/pub/docs/workshops/99_docs/46.pdf.

[7] Wessman, C. A, C. A. Bateson, B. Curtiss, and T. L. Benning,. "A Comparison of the Spectral Mixure Analysis and NDVI for Ascertaining Ecological Variables," AVIRIS Airborne Geoscience Workshop Proceedings, 1993, ftp://popo.jpl.nasa.gov/pub/docs/workshops/93_docs/48.pdf.

[8] G.A. Carter, "Ratios of leaf reflectance's in narrow wavebands as indicators of plant stress," International Journal of Remote Sensing, vol.15, pp. 697-703, 1994.

[9] G.A. Blackburn, "Spectral indices for estimating photosynthetic pigment concentrations: a test using senescent tree leaves," International Journal of Remote Sensing. vol. 19, pp. 657-675, 1998.

[10] T.P. Dawson and P.J. Curran, "A new technique for interpolating the reflectance red edge position," International Journal of Remote Sensing, vol. 19, pp. 2133-2139, 1998.

[11] T.G. Mueller, A.D. Karathanasis, P.L. Cornelius, and H. Cetin. "Hyperspectral Imagery: variability within and between soil map phases," Robert et al. (ed.) Proc. 6th international conference on precision Agriculture. ASA Misc. Publ., ASA, CSSA, and SSSA, Madison, WI. PDF-CD, 2002.

[12] K. McGwire, T. Minor, and L. Fenstermaker, "Hyperspectral Mixture Modeling for Quantifying Sparse Vegetation Cover in Arid Environments," Remote Sensing of Environment, vol. 72, pp. 360-374, 2000.

[13] N. Gat, H. Erives, G. J. Fitzgerarld, S. R. Kaffa, and S. J. Maas, "Estimating Sugar Beet Yields Using AVIRIS-Derived Indices," AVIRIS Airborne Geoscience Workshop Proceedings, 2000, ftp://popo.jpl.nasa.gov/pub/docs/workshops/00_docs/Gat_web.pdf.

[14] E. M. Perry, M. Gardner, J. Tagestad, D. Roberts, P. Cassidy, J. Smith, and D. Nichols, "Effects of Image Resolution and Uncertainties on Reflectance-Derived Crop Stress Indicators," AVIRIS Airborne Geoscience Workshop Proceedings, 2000, ftp://popo.jpl.nasa.gov/pub/docs/workshops/00_docs/perry_web.pdf.

[15] Z. Chen, C. D. Elvidge, and D. P. Groenveld, "Discrimination of Green Vegetation Cover Using a High Spectral Resolution Vegetation Index" AVIRIS Airborne Geoscience Workshop Proceedings, 1996, ftp://popo.jpl.nasa.gov/pub/docs/workshops/96_docs/4.pdf

[16] CSES (Center for the Study of Earth from Space), "Atmospheric REMoval Program (ATREM), version 3.0," University of Colorado, Boulder, CO., 1997.

[17] RSI (Research Systems Inc.), "The Environment for Visualizing Images (ENVI) Version 3.4," Boulder, CO., 2000.

[18] D.G. Kleinbaum, L.L. Kupper, K.E. Muller, and A. Nizam, "Applied Regression Analysis and Other Multivariable Methods," Brooks/Cole Publishing, Pacific Grove, CA., 1998